Theoretical study of four-probe resistance in nanoscale measurements: Monatomic carbon chains and (5,5)-carbon nanotubes

Asako Terasawa,* Tomofumi Tada, and Satoshi Watanabe
Department of Materials Engineering, University of Tokyo, 7-3-1 Hongo, Bunkyo-ku, Tokyo 113-8656, Japan
and CREST, Japan Science and Technology Agency, 4-1-8 Honcho Kawaguchi, Saitama 322-0012, Japan
(Received 9 September 2008; revised manuscript received 6 May 2009; published 28 May 2009)

Simulations of four-probe resistance measurements of monatomic carbon chains and (5,5)-carbon nanotubes were carried out using the self-consistent charge density-functional tight-binding method and the Green's function method. The four-probe resistance spectra show oscillations depending on the probe geometries and become negative at specific electron energies. These features coincide qualitatively with those experimentally observed by Gao *et al.* [Phys. Rev. Lett. **95**, 196802 (2005)]. It is shown that the resistance oscillations can be attributed to the interference of electron waves between the two voltage probes.

DOI: 10.1103/PhysRevB.79.195436 PACS number(s): 73.63.Fg, 05.60.Gg, 73.22.−f

I. INTRODUCTION

The measurement of transport properties through molecules and nanostructures has become one of the most important topics in nanoscale technology and physics. In such measurements, contact resistance between the sample and probes often prevents clarification of the intrinsic transport properties of the sample. Recently, it becomes possible to apply the four-probe method, which is a well-known and well-established technique used to eliminate the contact resistance to nanoscale systems owing to the development of novel techniques such as independently driven probes of a scanning tunneling microscope (STM).[1–7] In a four-probe measurement using STM tips of a PtIr-coated multiwall carbon nanotube (MWNT), the minimum probe spacing was reduced to approximately 30 nm.[8] The four-probe method is, however, based on the transport model in the macroscale, and its applicability to microscopic systems is not guaranteed. In fact, it has been pointed out that quantum interference may make the interpretation of four-probe resistance difficult.[9] For example, Zhang and Chandrasekhar[10] reported that the quantum interference effect in MWNT is observed in four-probe measurements. In addition, a few recent experiments have reported anomalous behavior of four-probe resistance. Gao *et al.*[11] reported fine oscillations of four-probe resistance for a single-wall carbon nanotube (SWNT) using a sweeping gate voltage at cryogenic temperatures. They also observed that the four-probe resistance of SWNT sometimes becomes negative and reaches $-0.6R_{2\mathrm{pt}}$ at minimum, where $R_{2\mathrm{pt}}$ is the two-probe resistance of the same system.

On the other hand, quantum effects on resistance oscillation of atomic chain have been studied theoretically and experimentally for many years. For example, Lang and Avouris[12,13] reported the conductance oscillation of atomic chain depending on the number of atoms in the chain, and Smit *et al.*[14] observed the same behavior experimentally. Also, Thygesen and Jacobsen[15] reported the computational analysis of conductance oscillation of atomic chain with respect to the electron energy. They pointed out the relation between the conductance oscillation and the matching of the levels of atomic chain to the Fermi level of electrodes. However, it is still unclear whether the resistance oscillation in the experiment of carbon nanotubes can be understood from the ideas proposed in the above studies straightforwardly. In addition, the negative resistance observed in the experiment cannot be interpreted by the two-probe calculations in the previous studies: the negative differential resistance studied in two-probe systems[16] is essentially different from the negative four-probe resistance.[17]

Theoretical studies on multiprobe transport of nanoscale order have also been reported. For example, Kobayashi[18,19] examined surface-state conduction. However, the multiprobe calculations in previous studies are based on empirical parameters, and the effects of charge redistribution at surfaces and probe-sample contacts are not taken into account. Thus theoretical analyses based on more reliable methods are highly desirable for a deeper understanding of the interference effects in nanoscale four-probe measurements and the extraction of information regarding the intrinsic transport properties of nanostructures from four-probe measurements.

Considering these influencing factors, we have developed a simulator for multiprobe transport measurements. In this paper, we present computational results of four-probe resistance for two systems: a monatomic carbon chain and a (5,5)-CNT under low bias and at the low-temperature limit. In these results, we found the oscillations of four-probe resistances and the negative four-probe resistances which depend on the sample-probe geometry and that these behaviors can be interpreted by the interference of multiple reflected electron waves between sample and probes. We show that the present results are qualitatively consistent with a previous observation[11] and our approach is promising for detailed analyses of four-probe resistance in nanoscale measurements.

II. CALCULATION METHODS

The four-probe resistance in the coherent transport regime is considered. The current flowing from probe p to the sample can be expressed on the basis of the Landauer-Büttiker formula[9] as follows:

$$I_p = -\frac{2e}{h}\sum_{q=1}^{4}\left[\int T_{qp}(E)f(E-\mu_p)dE - \int T_{pq}(E)f(E-\mu_q)dE\right], \quad (1)$$

where T_{pq} is the transmission coefficient between probes p and q and μ_p is the chemical potential of probe p. At low bias and the low-temperature limit, Eq. (1) can be simplified to the following matrix equation:

$$\begin{Bmatrix} V_1 - V_4 \\ V_2 - V_4 \\ V_3 - V_4 \end{Bmatrix} = \frac{h}{2e^2}\bar{\mathbf{T}}^{-1}\begin{Bmatrix} I_1 \\ I_2 \\ I_3 \end{Bmatrix}. \quad (2)$$

$\bar{\mathbf{T}}$ is a 3×3 matrix of which the element can be written as $\bar{T}_{pq}=-T_{pq}+\delta_{pq}\Sigma_{r=1}^{4}T_{pr}$ and V_p is the bias voltage applied to probe p, which corresponds to the electrochemical potential μ_p as $\mu_p-\mu_0=-eV_p$. In four-probe measurements, the condition $I_2=I_3=0$ is imposed. Under this condition, the two-probe resistance R_{2pt} and the four-probe resistance R_{4pt} in the coherent region can be represented as

$$\begin{aligned} R_{2pt} &= \frac{V_1 - V_4}{I_1} \\ &= \frac{h}{2e^2}[\bar{\mathbf{T}}^{-1}]_{11} \\ &= \frac{h}{2e^2}\frac{(T_{12}+T_{42})(T_{13}+T_{43}+T_{23})+T_{32}(T_{13}+T_{43})}{\det[\bar{\mathbf{T}}]} \end{aligned} \quad (3)$$

and

$$\begin{aligned} R_{4pt} &= \frac{V_2 - V_3}{I_1} \\ &= \frac{h}{2e^2}[(\bar{\mathbf{T}}^{-1})_{21}-(\bar{\mathbf{T}}^{-1})_{31}] \\ &= \frac{h}{2e^2}\frac{T_{12}T_{43}-T_{13}T_{42}}{\det[\bar{\mathbf{T}}]}. \end{aligned} \quad (4)$$

The Green's function method was adopted to calculate the density matrices and transmission coefficients of four-probe systems. The overlap matrix $\mathbf{S}$ and the Hamiltonian matrix $\mathbf{H}$ appearing in the Green's function $\mathbf{G}=[E\mathbf{S}-\mathbf{H}-\Sigma]^{-1}$ and the self-energy Σ are calculated using the self-consistent charge density-functional tight-binding (SCC-DFTB) method.[20–22] This method is an approximate expression of the density-functional theory (DFT) in the framework of the tight-binding method. In the DFTB method, atomic orbitals are determined from atomic DFT calculations, and the distance-dependent terms of the Hamiltonian and overlap matrices are calculated within a two-center approach using the atomic orbitals. The effect of polarization on total energy is taken into account in a self-consistent scheme based on Mulliken charges. Note that the present self-consistent scheme is essentially the same as the one often adopted in nanoscale conductance calculations.[23]

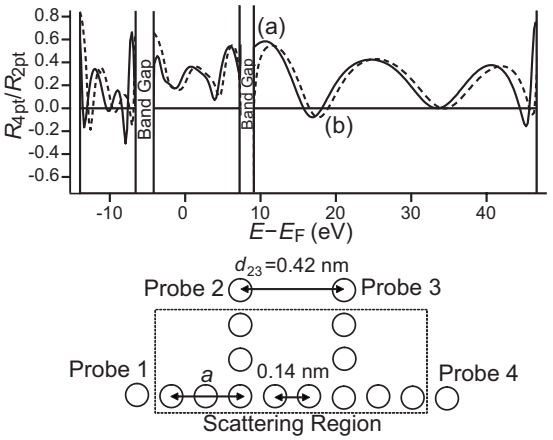

FIG. 1. R_{4pt}/R_{2pt} spectra for the monatomic carbon chain system schematically shown in the lower figure, obtained from (a) self-consistent calculation (solid line) and (b) non-self-consistent calculation (dashed line). The region indicated by the dotted rectangle denotes the scattering region where the Green's function is calculated self-consistently. The vector a is the primitive translation vector adopted in drawing the band structure of the monatomic carbon chain shown in Fig. 5.

The self-energy matrices of probes were calculated with the mode-matching method proposed by Ando.[24,25] In the mode-matching method, self-energies are obtained as displacement operators for the wave functions in one-dimensional periodic probes. This method requires only one matrix equation to obtain a self-energy and thus takes much less time than other approaches such as the recursion method.[26] In the present study, systems consisting of only carbon atoms were examined. The parameters developed by Porezag *et al.*[20] were adopted for the SCC-DFTB calculations.

III. RESULTS AND DISCUSSION

A. Four-probe resistance of monatomic carbon chain

First, a system consisting of a sample of monatomic carbon chain and probes of semi-infinite monatomic carbon chains was examined as mentioned previously. Figure 1 shows the calculated spectra for four-probe resistance divided by two-probe resistance as a function of the electron energy, together with the monatomic configuration adopted in the calculation. Note that the change in electron energy corresponds to the change in gate bias voltage in experiments because the Fermi level of the system can be modulated by application of a gate bias. The solid and dashed lines in the graph represent the R_{4pt}/R_{2pt} spectra obtained from self-consistent and non-self-consistent calculations, respectively. The important features seen in these spectra are the oscillatory behavior of R_{4pt}/R_{2pt} and the appearance of negative values of R_{4pt}/R_{2pt}. These features are in common with the self-consistent and non-self-consistent calculations. The only difference between the two calculations is found in the shift of the spectra by 0.2–1.3 eV.

Let us consider the origin of the oscillatory behavior of R_{4pt}/R_{2pt}. Figure 2 shows the spectra of R_{4pt}/R_{2pt}, R_{4pt}, and

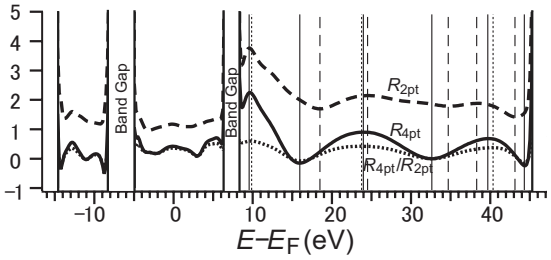

FIG. 2. Spectra of R_{4pt}/R_{2pt} (dotted), R_{4pt} (solid), and R_{2pt} (dashed) with respect to the energy of incident electrons at $d_{23}=0.42$ nm. The thin dotted, solid, and dashed vertical lines represent the energies where respective spectra take their extremal values.

R_{2pt} of the same system as in Fig. 1. We can see similar oscillatory behaviors in all the spectra of R_{4pt}, R_{4pt}/R_{2pt}, and R_{2pt}. However, we would like to point out two important features. First, the amplitudes of oscillation are much smaller in R_{2pt} than in R_{4pt}. Second, the oscillation period is the same between R_{4pt} and R_{4pt}/R_{2pt}, while it is a little different in R_{2pt}. The difference is clearly seen, for example, in the range from 9.0 to 46.0 eV, where the energies corresponding to the extremal values are sometimes different between the R_{4pt} and R_{2pt} spectra. Thus we can say that the behavior of R_{4pt}/R_{2pt} is determined mainly by the behavior of R_{4pt} rather than that of $1/R_{2pt}$.

In Fig. 3, the R_{4pt}/R_{2pt} spectra are compared at different sample-probe distances: $d_{t\text{-}s}$ of 0.14 and 0.28 nm. Here, the distance between probe 3 and the sample is set to be the same as that between probe 2 and the sample. It can be seen from this figure that the four-probe resistance oscillates much more strongly at $d_{t\text{-}s}=0.14$ nm than at $d_{t\text{-}s}=0.28$ nm. This can be understood to be due to much weaker interactions between the probe and sample in the latter case.

The dependence of the four-probe resistance spectra on the probe spacing d_{23} was also examined. Figure 4 shows the energy spectra of R_{4pt}/R_{2pt} at different probe spacings: $d_{23}=0.42$, 0.56, and 0.70 nm. The tip-sample distance $d_{t\text{-}s}$ was set to be 0.14 nm. The characteristic pattern of resistance oscillation appears at each probe spacing and the periods of

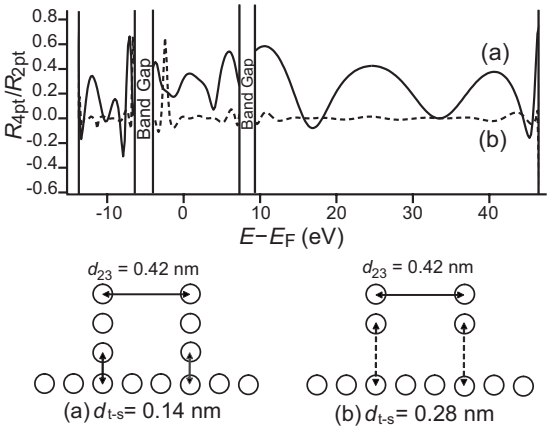

FIG. 3. R_{4pt}/R_{2pt} spectra for the monatomic carbon chain at different tip-sample distances, (a) $d_{t\text{-}s}=0.14$ nm (solid line) and (b) $d_{t\text{-}s}=0.28$ nm (dashed line).

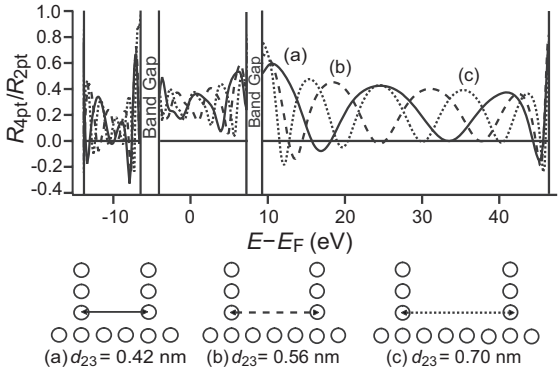

FIG. 4. R_{4pt}/R_{2pt} spectra for the monatomic carbon chain at different probe spacings: (a) $d_{23}=0.42$ nm (solid line), (b) $d_{23}=0.56$ nm (dashed line), and (c) $d_{23}=0.70$ nm (dotted line).

oscillation become smaller with the increase in d_{23}. These results show that this oscillatory behavior is caused by the contacts between the sample and the voltage probes (probes 2 and 3). By comparing these spectra with the band structure of the carbon chain shown in Fig. 5, it was found that R_{4pt}/R_{2pt} takes local minima and maxima when d_{23} satisfies $d_{23}=n\lambda/2$ and $d_{23}=(2n+1)\lambda/4$, respectively.

This oscillatory feature looks similar to the even-odd behavior of conductance seen in the previous studies of monatomic chain[12–15] such that the conductance oscillates as a function of the length. However, the negative value of R_{4pt}/R_{2pt} at some of the minimum points cannot be interpreted with the simple model of resonant tunneling at the eigenstates of monatomic chain proposed in the previous studies. To understand this, we introduced a simple phase-coherent model of four-probe system shown in Fig. 6. We considered the phase shifts between directly transmitted waves and the waves transmitted after one reciprocation between voltage probes (probes 2 and 3) in both of the figures. When $d_{23}=n\lambda/2$, destructive interference occurs between the electron waves flowing through probe 2 to probe 1 directly

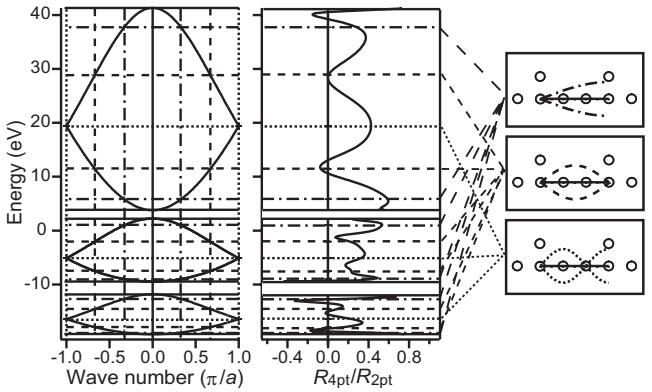

FIG. 5. Comparison of the band structure of the monatomic carbon chain and the four-probe resistance spectra at $d_{23}=0.42$ nm. The dotted, dashed, and chained lines represent the energies where the wave vectors take the values of $\pm\pi/a$, $\pm 2\pi/3a$, and $\pm\pi/3a$, respectively. (Note that the primitive translation vector a is set to be twice as long as the bond length, that is, $a=0.28$ nm.)

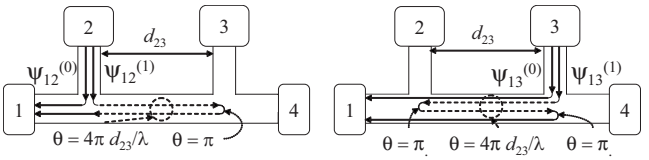

FIG. 6. A schematic of phase-coherent scattering between probe 2 and probe 3. In each case, the phase shift caused by the path difference is $4\pi d_{23}/\lambda$ and a phase shift per one reflection is π. When $d_{23}=n\lambda/2$, the total phase shifts become π in the left figure and 2π in the right figure.

and those via the contact of probe 3, while constructive interference occurs between the electron waves flowing through probe 3 to probe 1 directly and those reflected between probes 2 and 3. These interferences can lead to the smaller transmission coefficient between probes 1 and 2, T_{12}, compared with the one between probes 1 and 3, T_{13}. As can be seen from Eq. (4), this corresponds to the negative four-probe resistance, though actual situation is more complicated due to the existence of other waves.

B. Four-probe resistance of (5,5)-carbon nanotube

Next, a four-probe measurement was examined for a more complicated structure, which consists of (5,5)-carbon nanotubes. It should be noted that non-self-consistent calculations were performed for this system to save computational time. Judging from the difference between the self-consistent and non-self-consistent calculations in the case of the monatomic chain system, it is expected that semiquantitative analyses are possible using non-self-consistent results. Figure 7 shows the geometry of the four-probe model consisting of (5,5)-CNTs and the R_{4pt}/R_{2pt} spectra of (5,5)-CNT at tip-sample distances $d_{t\text{-}s}$ of 0.14 and 0.28 nm. Oscillatory behavior and negative resistance were again obtained. The minimum four-probe resistance reaches approximately $-0.2R_{2pt}$ around the Fermi level at $d_{t\text{-}s}=0.14$ nm. The magnitude of R_{4pt}/R_{2pt} at $d_{t\text{-}s}=0.28$ nm is much smaller than at $d_{t\text{-}s}=0.14$ nm for the

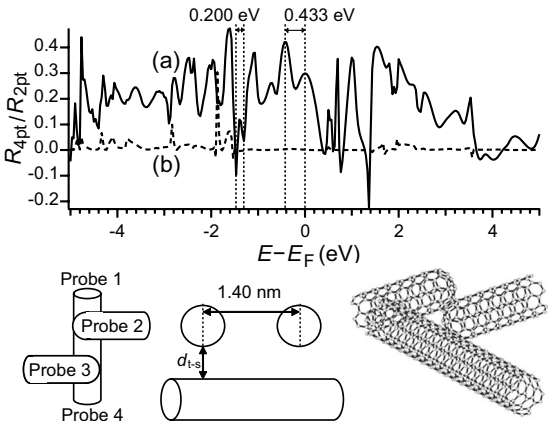

FIG. 7. Four-probe model consisting of (5,5)-CNTs and R_{4pt}/R_{2pt} spectra for this model with different tip-sample distances: (a) $d_{t\text{-}s}=0.14$ nm (solid line) and (b) $d_{t\text{-}s}=0.28$ nm (dashed line). The tips of the (5,5)-CNTs are terminated with hemispherical fullerene structures consisting of 30 carbon atoms.

energy range investigated, except for several peaks of resistances, as in the case of the monatomic chain. The fine and complicated oscillation of four-probe resistance at $d_{t\text{-}s}=0.14$ nm clearly originates from interference effects, as was the case for the results of monatomic chains.

To compare the periods of resistance oscillation in our models ($d_{23}=1.40$ nm) with those observed experimentally by Gao *et al.*[11] ($d_{23}=140$ nm), a roughly approximated relation was derived between the period of resistance oscillation ΔE and the probe spacing d_{23} as follows. From Fig. 4, it can be seen that the numbers of peaks of R_{4pt}/R_{2pt} per energy band are 3, 4, and 5 at $d_{23}=0.42$ nm, $d_{23}=0.56$ nm, and $d_{23}=0.70$ nm, respectively. Therefore the number of peaks N_P can be written approximately as

$$N_P = \frac{d_{23}\ (\text{nm})}{0.14\ (\text{nm})}. \tag{5}$$

Note that 0.14 nm is the bond length of the carbon chain. Assuming that the peak spacing is almost uniform in a whole band, the period of resistance oscillation ΔE can be expressed as

$$\Delta E = \frac{E_{\text{top}} - E_{\text{bottom}}}{d_{23}/0.14},$$

where $E_{\text{top}}-E_{\text{bottom}}$ represents the width of the energy band. Since the width of the energy band crossing the Fermi level can be estimated as 11.39 eV from the calculated band structure shown in Fig. 5, we obtain

$$\Delta E\ (\text{eV}) = \frac{1.59\ (\text{eV nm})}{d_{23}\ (\text{nm})} \tag{6}$$

for the monatomic chain system. It is expected that rough estimates using Eq. (6) are possible for more complicated systems, although the peaks do not necessarily appear uniformly, and the band structure must be much more complicated than that of a monatomic carbon chain. In fact, using this relation for the four-probe model of (5,5)-CNT with $d_{23}=1.40$ nm, the oscillation period ΔE is estimated as 1.1 eV. This value approximately coincides with $\Delta E=0.2-0.5$ eV around the Fermi level estimated from the numerical results given in Fig. 7. Thus, it is expected that this approach would be applicable for an approximated analysis of complex systems. Using Eq. (6), the period of oscillation is calculated as 11 meV for the case of $d_{23}=140$ nm. This value is comparable to the experimental result reported by Gao *et al.*,[11] $\Delta V_g \sim 10$ mV at $d_{23}=140$ nm. This suggests that the resistance oscillation seen in their measurement can be attributed to the interference of electron waves between the voltage probes. On the other hand, discrepancies between our calculation and their experiment results are also noticed. For example, the absolute value of R_{4pt}/R_{2pt} in their experiment sometimes exceeds the maximum obtained from our calculation considerably, and the energy range where the negative resistance is observed seems wider in their experiment than in our calculation. The factors neglected in our calculation such as structural relaxation, defects, and applied bias voltage may be crucial to understand the origin of these

quantitative discrepancies, and thus, further detailed analyses are required.

IV. SUMMARY

A multiprobe transport simulation program was developed based on the self-consistent charge density-functional tight-binding method and the Green's function method, and the four-probe resistance of a monatomic carbon chain and a (5,5)-CNT were examined using this program. It was found that the four-probe resistance of a monatomic carbon chain oscillates by sweeping the energy of incident electrons, and the four-probe resistance becomes negative at specific energies. We have revealed that this resistance oscillation is caused by the interference of electron waves between the two voltage probes. For the (5,5)-CNT models, the resistance oscillation patterns become fine and complicated, and the calculated minimum four-probe resistance reaches $-0.2R_{2pt}$. From an approximate relationship between the oscillation period of the four-probe resistance and the probe spacing derived from the results of the monatomic chain model, it was shown that the oscillatory behavior observed by Gao *et al.* can also be attributed to the interference effect.

ACKNOWLEDGMENTS

We thank Takahiro Yamamoto and Satofumi Souma for helpful discussions and Hiroyuki Kageshima for discussions and continuous support. This work was partially supported by Grant-in-Aid for Scientific Research on Priority Areas, "Nano-linked molecule (448)," under Grant No. 20027003 and for Scientific Research under Grant No. 20360016 from the Ministry of Education, Culture, Sports, Science and Technology (MEXT) of Japan.

*asako@cello.t.u-tokyo.ac.jp

[1] S. Hasegawa, J. Phys.: Condens. Matter **12**, R463 (2000).
[2] I. Shiraki, T. Nagao, S. Hasegawa, C. L. Petersen, P. Bøggild, T. M. Hansen, and F. Hansen, Surf. Rev. Lett. **7**, 533 (2000).
[3] C. L. Petersen, F. Gray, I. Shiraki, and S. Hasegawa, Appl. Phys. Lett. **77**, 3782 (2000).
[4] I. Shiraki, F. Tanabe, R. Hobara, T. Nagao, and S. Hasegawa, Surf. Sci. **493**, 633 (2001).
[5] S. Hasegawa, I. Shiraki, F. Tanabe, and R. Hobara, Curr. Appl. Phys. **2**, 465 (2002).
[6] S. Hasegawa, I. Shiraki, T. Tanikawa, C. L. Petersen, T. M. Hansen, P. Böggid, and F. Gray, J. Phys.: Condens. Matter **14**, 8379 (2002).
[7] S. Hasegawa, I. Shiraki, F. Tanabe, R. Hobara, T. Kanagawa, T. Tanikawa, and I. Matsuda, Surf. Rev. Lett. **10**, 963 (2003).
[8] S. Yoshimoto, Y. Murata, K. Kubo, K. Tomita, K. Motoyoshi, T. Kimura, H. Okino, R. Hobara, I. Matsuda, S. Honda, M. Katayama, and S. Hasegawa, Nano Lett. **7**, 956 (2007).
[9] S. Datta, *Electronic Transport in Mesoscopic Systems* (Cambridge University Press, New York, 1995).
[10] Z. Zhang and V. Chandrasekhar, Phys. Rev. B **73**, 075421 (2006).
[11] B. Gao, Y. F. Chen, M. S. Fuhrer, D. C. Glattli, and A. Bachtold, Phys. Rev. Lett. **95**, 196802 (2005).
[12] N. D. Lang, Phys. Rev. Lett. **79**, 1357 (1997).
[13] N. D. Lang and Ph. Avouris, Phys. Rev. Lett. **81**, 3515 (1998).
[14] R. H. M. Smit, C. Untiedt, G. Rubio-Bollinger, R. C. Segers, and J. M. van Ruitenbeek, Phys. Rev. Lett. **91**, 076805 (2003).
[15] K. S. Thygesen and K. W. Jacobsen, Phys. Rev. Lett. **91**, 146801 (2003).
[16] K. H. Khoo, J. B. Neaton, Y. W. Son, M. L. Cohen, and S. G. Louie, Nano Lett. **8**, 2900 (2008).
[17] For example, the negative four-probe resistance implies that the polarity of the voltage between the voltage probes is opposite to that between the outside current probes, while such reversal of voltage polarity does not appear in the case of the negative differential resistance in two-probe systems.
[18] K. Kobayashi, Phys. Rev. B **65**, 035419 (2002).
[19] K. Kobayashi, Surf. Sci. **583**, 16 (2005).
[20] D. Porezag, Th. Frauenheim, Th. Köhler, G. Seifert, and R. Kaschner, Phys. Rev. B **51**, 12947 (1995).
[21] M. Elstner, D. Porezag, G. Jungnickel, J. Elsner, M. Haugk, Th. Frauenheim, S. Suhai, and G. Seifert, Phys. Rev. B **58**, 7260 (1998).
[22] Th. Frauenheim, G. Seifert, M. Elstner, Z. Hajnal, G. Jungnickel, D. Porezag, S. Suhai, and R. Scholz, Phys. Status Solidi B **217**, 41 (2000).
[23] M. Brandbyge, J.-L. Mozos, P. Ordejón, J. Taylor, and K. Stokbro, Phys. Rev. B **65**, 165401 (2002).
[24] T. Ando, Phys. Rev. B **44**, 8017 (1991).
[25] P. A. Khomyakov, G. Brocks, V. Karpan, M. Zwierzycki, and P. J. Kelly, Phys. Rev. B **72**, 035450 (2005).
[26] F. Guinea, C. Tejedor, F. Flores, and E. Louis, Phys. Rev. B **28**, 4397 (1983).